Neuron, Vol. 36, 891–896, December 5, 2002, Copyright ©2002 by Cell Press

Rod Cyclic Nucleotide-Gated Channels Have a Stoichiometry of Three CNGA1 Subunits and One CNGB1 Subunit

Jie Zheng, Matthew C. Trudeau, and William N. Zagotta[1]
Howard Hughes Medical Institute
Department of Physiology and Biophysics
Box 357290
University of Washington School of Medicine
Seattle, Washington 98195

Summary

Phototransduction relies on the precise balance of speed and sensitivity to achieve optimal performance. The cyclic nucleotide-gated (CNG) ion channels, with their Ca^{2+} permeability, high sensitivity to changes in cytosolic cGMP, rapid gating kinetics, and Ca^{2+}-calmodulin modulation, are beautifully optimized for their role in light detection. Many of these specializations come about from the heteromeric composition of the native channel, comprised of CNGA1 and CNGB1 subunits. However, the stoichiometry and arrangement of these subunits is unknown. Here we have used an approach based on fluorescence resonance energy transfer (FRET) to determine the composition of the intact functional channel in the surface membrane. We find, surprisingly, that the channel contains three CNGA1 subunits and only one CNGB1 subunit. These results have implications for CNG channel function in particular and assembly of membrane proteins in general.

Introduction

CNG channels are members of the voltage-activated family of channels (Zagotta and Siegelbaum, 1996). Like the voltage-activated K^+ channels, CNG channels are composed of four subunits around an aqueous pore. Each subunit contains six transmembrane segments (S1–S6) and a pore-forming P loop between S5 and S6. In addition, each subunit contains a cyclic nucleotide binding domain in the carboxy-terminal region. While several of the CNG channel subtypes express functionally as homomers in exogenous expression systems, all of the native channels that have been identified to date are heteromeric, composed of two or three different subunit types (Bonigk et al., 1999; Bradley et al., 1994, 1997, 2001; Chen et al., 1993, 1994; Korschen et al., 1995; Liman and Buck, 1994; Munger et al., 2001; Sautter et al., 1998). The native CNG channel in rod photoreceptors, in particular, contains both CNGA1 (formerly CNG1; Rod α) and CNGB1 (formerly CNG4; Rod β) subunits (Chen et al., 1993, 1994; Kaupp et al., 1989; Korschen et al., 1995). While the CNGA1 subunit can form functional homomeric channels, the CNGB1 subunit alone is not functionally expressed at the membrane surface (Chen et al., 1993; Kaupp et al., 1989). However, when coexpressed with the CNGA1 subunit, the CNGB1 subunit is coassembled into heteromeric channels that are trafficked to the surface and functional. The CNGB1 subunit confers several novel properties to the heteromeric channels, including altered permeation and block by Ca^{2+}, more rapid single-channel kinetics, a 10-fold increase in the current activated by cAMP, modulation by Ca^{2+}-calmodulin (Ca^{2+}/CaM), and sensitivity to L-*cis* diltiazem (Bauer, 1996; Chen et al., 1993, 1994; Hsu and Molday, 1993, 1994; Korschen et al., 1995; Shammat and Gordon, 1999). These properties closely mirror the properties of native rod CNG channels (Yau and Baylor, 1989).

While the composition of the native rod channel is well established, the stoichiometry of the different subunits is not. Two different studies have reported a stoichiometry of 2 CNGA1 subunits and 2 CNGB1 subunits, though with differing arrangements (He et al., 2000; Shammat and Gordon, 1999). To determine the stoichiometry of the heteromeric channels more directly, we have used an approach based on fluorescence resonance energy transfer (FRET). FRET reports the proximity of two fluorophores (Selvin, 1995). Light energy absorbed by a donor fluorophore is transferred to a nearby acceptor fluorophore whose absorption spectrum overlaps the emission spectrum of the donor. The efficiency of energy transfer falls off with the sixth power of the distance between the donor and acceptor molecules, making FRET a sensitive reporter of proximity.

For these experiments, the donor fluorophore (eCFP) and acceptor fluorophore (eYFP) were genetically attached to the carboxyl or amino terminus of different CNG channel subunits. The fluorescent proteins eCFP and eYFP have previously been shown to function as a FRET pair with a distance for 50% transfer efficiency (Ro) of approximately 50 Å (Miyawaki et al., 1997; Patterson et al., 2000). This distance makes them optimal for reporting the presence of two fluorophore-containing subunits in the same channel. To determine the stoichiometry of the heteromeric channels, we have performed two sets of experiments (Figure 1A). To test for the presence of two or more CNGA1 subunits in the heteromeric channel, we have coexpressed CNGA1-eCFP, CNGA1-eYFP, and CNGB1 in *Xenopus* oocytes (Figure 1A, left). The presence of a FRET signal (red arrows) indicates the occurrence of both CNGA1-eCFP and CNGA1-eYFP in the same channel. Similarly, to test for the presence of two or more CNGB1 subunits, we have coexpressed CNGA1, CNGB1-eCFP, and CNGB1-eYFP (Figure 1A, right). Since the channel is known to be a tetramer and homomeric channels do not form appreciably under our conditions (see below), these experiments are sufficient to establish the stoichiometry of the heteromeric channel. FRET in only the first experiment indicates a stoichiometry of 3 CNGA1 : 1 CNGB1. FRET in only the second experiment indicates a stoichiometry of 1 CNGA1 : 3 CNGB1. FRET in both experiments indicates a stoichiometry of 2 CNGA1 : 2 CNGB1.

Results and Discussion

The fluorescence signal from fluorophore-containing channels expressed in *Xenopus* oocytes was measured

[1]Correspondence: zagotta@u.washington.edu

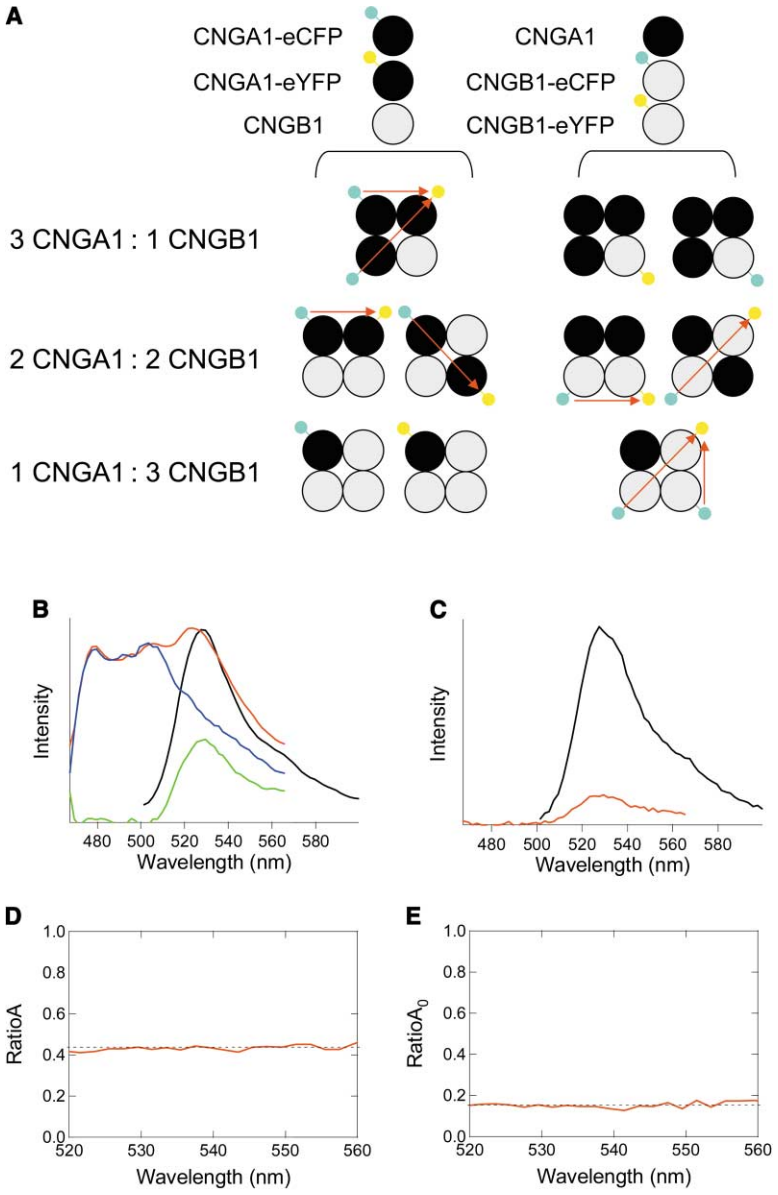

Figure 1. Determination of Channel Stoichiometry with FRET

(A) Possible stoichiometries and prediction for FRET. The CNGA1 subunits are black, the CNGB1 subunits are gray, the eCFP is cyan, and the eYFP is yellow. FRET is indicated by a red arrow.

(B and C) Spectral quantification of FRET efficiency. Emission spectra measured from oocytes expressing CNGA1-eCFP and eYFP-CNGB1 (B) and CNGA1-eYFP (C) are color coded as follows: red, 458 nm excitation; black, 488 nm excitation; blue, eCFP emission spectrum from CNGA1-eCFP; green, subtracted spectrum (difference between red and blue).

(D and E) RatioA (D) and $RatioA_0$ (E) as functions of wavelength.

using confocal microscopy. This approach has the advantage that fluorescence could be measured from only the surface membrane where mature, properly assembled channels were located. FRET was measured as emission of the acceptor (eYFP) during donor (eCFP) excitation with a 458 nm laser (Figure 1B, red line). Because of overlap in the eCFP and eYFP spectra, however, the measured eYFP emission due to FRET is always contaminated by both direct excitation of eYFP at 458 nm and by eCFP emission in the eYFP range. To overcome this problem, we quantified FRET efficiency using a spectrum approach (Figure 1B) that eliminated these contaminations as well as errors due to differences in channel density across experiments (Clegg, 1992; Selvin, 1995). The eYFP emission spectrum was extracted by subtracting the eCFP component using a scaled eCFP spectrum collected from control oocytes expressing only eCFP-tagged channels (CNGA1-eCFP) (Figure 1B, blue line). The ratio of the extracted spectrum (F458, green line) to the eYFP spectrum from the same oocyte with direct excitation with a 488 nm laser (F488, black line) was calculated as RatioA (Figure 1D). RatioA was independent of wavelength, confirming that the eCFP component was properly subtracted, and we were operating in the linear range of the detector. The RatioA component due to direct excitation of eYFP ($RatioA_0$) was measured directly from control oocytes expressing only eYFP-tagged channels (CNGA1-eYFP) (Figures 1C and 1E) and subtracted from RatioA, yielding a value ($RatioA - RatioA_0$) that was directly proportional to FRET efficiency.

The results of the experiments outlined above are shown in Figure 2. Coexpression of CNGA1-eCFP, CNGA1-eYFP, and CNGB1 produced a significant FRET signal, with an efficiency similar to coexpression of CNGA1-eCFP and CNGA1-eYFP alone (Figure 2). The FRET efficiency was similar over a range of expression levels, suggesting that FRET occurred between CNGA1 subunits in the

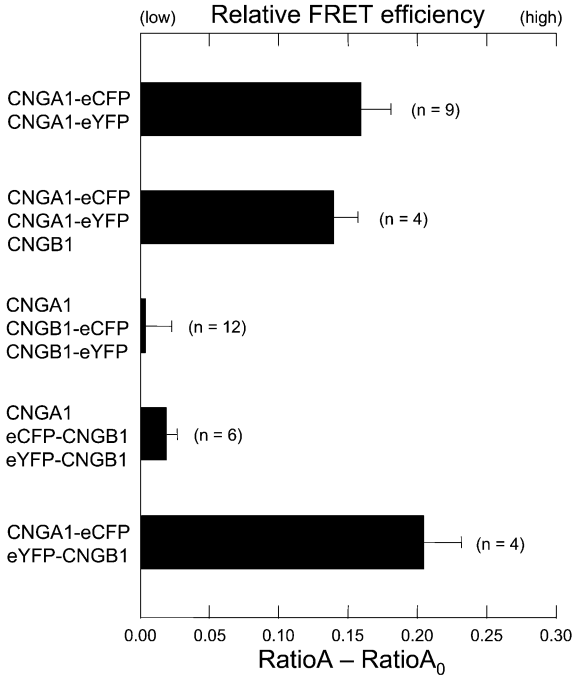

Figure 2. Summary of FRET Efficiency Measurements

Mean values of (RatioA − $RatioA_0$) and SEM are shown, with the number of measurements given in parentheses. These values are proportional to the FRET efficiency.

same channel as opposed to CNGA1 subunits in different channels (data not shown). Figure 3 shows that these heteromeric channels have the expected composition. The presence of both CNGA1-eCFP and CNGA1-eYFP is indicated by the high levels of fluorescence seen with direct excitation of eCFP (458 nm) and eYFP (488 nm) (Figure 3A). In addition, the presence of the CNGB1 subunit in the heteromeric channels is indicated by functional measurements. These heteromeric channels exhibited a high cAMP efficiency relative to homomeric CNGA1 channels (Shammat and Gordon, 1999; Trudeau and Zagotta, 2002a) and are modulated by Ca^{2+}/CaM unlike the homomeric channels (Figures 3B and 3C, Table 1; Chen et al., 1994; Trudeau and Zagotta, 2002b). These values of cAMP efficiency and Ca^{2+}/CaM modulation are similar to those reported for a homogeneous population of heteromeric channels (Shammat and Gordon, 1999; Trudeau and Zagotta, 2002b) and for native channels in rod photoreceptors (Table 1; Gordon et al., 1995; Picco et al., 1996; Rebrik and Korenbrot, 1998; Tanaka et al., 1989). Together, these results indicate that the heteromeric channel must contain at least two CNGA1 subunits.

Surprisingly, coexpression of CNGA1, CNGB1-eCFP, and CNGB1-eYFP did not produce a FRET signal significantly different from oocytes expressing eYFP-containing subunits alone. This is despite the fact that these oocytes showed significant levels of both CNGB1-eCFP and CNGB1-eYFP fluorescence and robust expression of functional heteromeric channels similar to coexpression of CNGA1-eCFP, CNGA1-eYFP, and CNGB1 (Figure 3, Table 1). These results suggest that the heteromeric rod channel only contains a single CNGB1 subunit.

For the experiments presented above, the fluorescent proteins were fused to the carboxyl terminus of the CNGA1 and CNGB1 subunits. We have repeated the experiments with the fluorescent proteins fused to the amino-terminal region of CNGB1, just N-terminal to the Ca^{2+}/CaM binding domain. As shown in Figure 2, coexpression of CNGA1, eCFP-CNGB1, and eYFP-CNGB1 also failed to show appreciable FRET despite showing significant levels of eCFP-CNGB1, and eYFP-CNGB1 fluorescence and heteromeric channel expression (Figure 3, Table 1). Furthermore, coexpression of CNGA1-eCFP and eYFP-CNGB1 produced a large FRET signal (Figure 2), showing that the eYFP-CNGB1 subunit is assembled into heteromeric channels and capable of producing FRET. The slightly larger FRET signal is consistent with the expectation that each eYFP-CNGB1 would be coassembled with three CNGA1-eCFP subunits. Consistent with this interpretation, coexpression of CNGA1-eYFP and eCFP-CNGB1 produced a smaller FRET signal (RatioA − $RatioA_0 = 0.12 \pm 0.017$ [n = 5]).

The absence of a FRET signal with the CNGB1 fusion proteins might result from an unfavorable distance or orientation between the fluorophores attached to CNGB1. This seems unlikely, however, for several reasons: (1) significant levels of FRET are seen between CNGA1 subunits and between CNGA1 and CNGB1 subunits, (2) the absence of FRET between CNGB1 subunits is observed with fluorophore attached to two different regions of CNGB1, (3) anisotropy measurements of eYFP-CNGB1 suggest that the fluorophores are highly mobile (data not shown), and (4) the channel is expected to be about 50 Å in diameter, and our FRET assay should be sensitive to distances of up to 80 Å. The absence of a FRET signal with the CNGB1 fusion proteins might also result if the CNGB1 fusion proteins expressed abundantly as monomers on the membrane surface. This is extremely unlikely given the robust FRET seen with coexpression of CNGA1-eCFP and eYFP-CNGB1 (Figure 2) and the lack of detectable surface expression of eYFP-CNGB1 alone (data not shown). These results indicate that the absence of a FRET signal with the CNGB1 fusion proteins did not result from an unfavorable distance or orientation between the fluorophores or monomer expression, but instead reflects the presence of only a single CNGB1 subunit in the heteromeric channel.

The occurrence of FRET between CNGA1 subunits but not between CNGB1 subunits leads to the clear and unexpected conclusion that the intact heteromeric channel has a stoichiometry of 3 CNGA1 subunits and 1 CNGB1 subunit. This conclusion is contrary to two earlier studies, using intersubunit metal coordination and tandem dimer constructs, that reported a stoichiometry of 2 CNGA1 subunits and 2 CNGB1 subunits (He et al., 2000; Shammat and Gordon, 1999). Furthermore, it is unexpected because the P loop-containing family of channels, of which CNG channels are a member, are generally thought to have a four-fold symmetric structure around the central pore (Doyle et al., 1998). It has also been suggested that CNG channels may function as a pair of dimers with two-fold axes of symmetry (Liu et al., 1998). However, the occurrence of only one CNGB1 subunit would constitute a break in both of these sym-

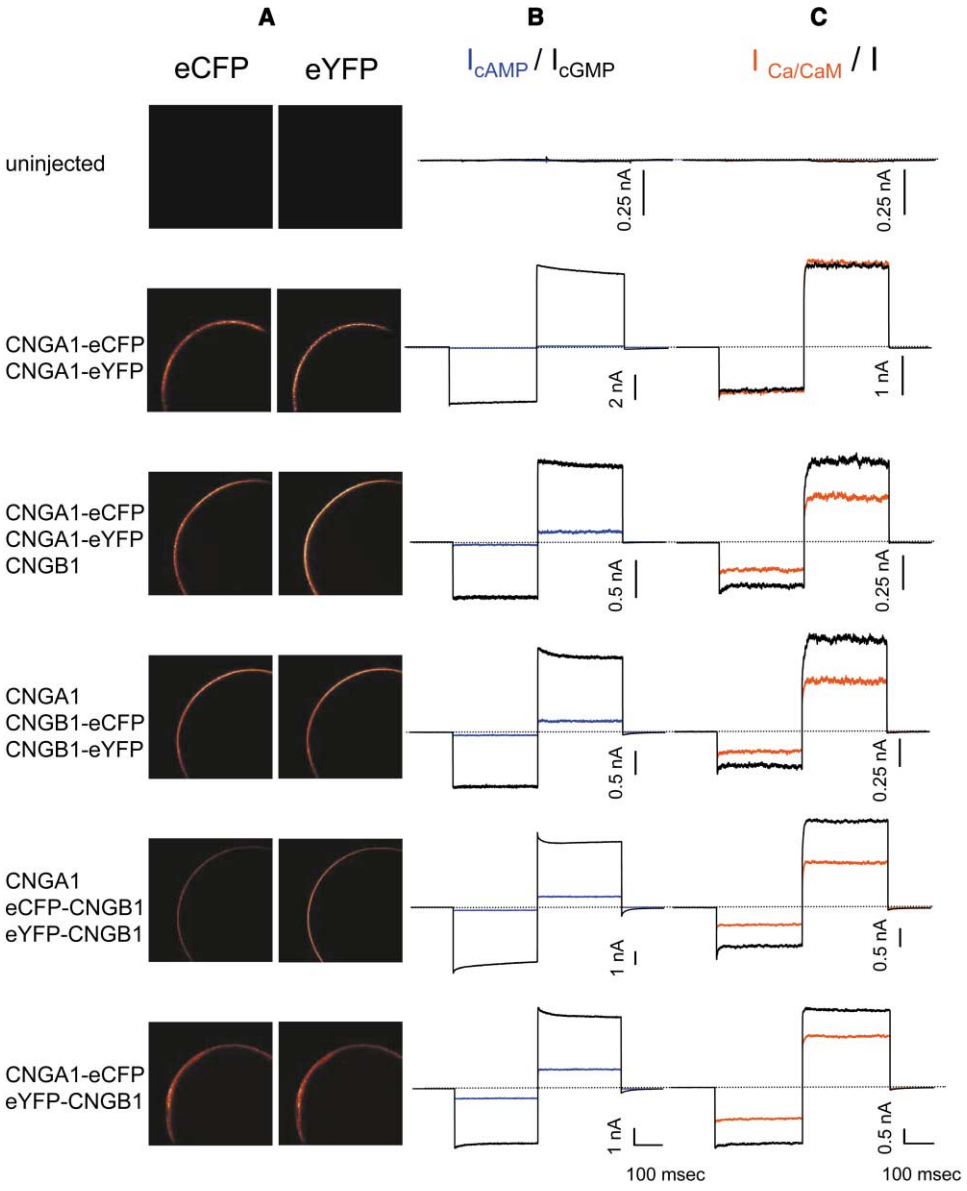

Figure 3. Confirmation of Channel Composition

(A) Pseudocolor images of oocytes showing eCFP fluorescence (excitation, 458 nm; emission, 485–490 nm) and eYFP fluorescence (excitation, 488 nm; emission, 525–530 nm).

(B) Currents activated by saturating (16 mM) cAMP (blue) and saturating (2.5 mM) cGMP (black) (I_{cAMP}/I_{cGMP}).

(C) Currents activated by subsaturating (30 μM) cGMP in the presence of Ca^{2+}/CaM (red) and in the absence of Ca^{2+}/CaM (black) ($I_{Ca/CaM}/I$).

metries. This break in symmetry also has profound implications for channel assembly and trafficking.

The CNGB1 subunit is directly responsible for many functional specializations of the rod channel, including altered permeation and block by Ca^{2+}, more rapid single-channel kinetics, a 10-fold increase in the current activated by cAMP, and modulation by Ca^{2+}/CaM (Bauer, 1996; Chen et al., 1993, 1994; Hsu and Molday, 1993, 1994; Korschen et al., 1995; Shammat and Gordon, 1999). It remains to be seen how a single subunit can produce such profound alterations in channel behavior.

Experimental Procedures

The bovine rod cyclic nucleotide-gated channel cDNAs for CNGA1 (formerly CNG1; Rod α) and CNGB1 (formerly CNG4; Rod β, kindly provided by R. Molday) (Korschen et al., 1995) used here were previously described (Trudeau and Zagotta, 2002a). eCFP (enhanced cyan fluorescent protein) and eYFP (enhanced yellow fluorescent protein; kindly provided by R. Tsien) (Miyawaki et al., 1997) were genetically attached to the carboxy-terminal end of both CNGA1 and CNGB1 subunits (denoted CNGA1-eCFP, CNGA1-eYFP, CNGB1-eCFP, and CNGB1-eYFP) and to the amino-terminal end of CNGB1 subunit after removing the glutamic acid-rich protein (GARP) sequence (amino acids 2–676) (denoted eCFP-CNGB1 and

Table 1. Properties of Wild-Type and eCFP- and eYFP-Containing CNG Channels

Channel	I_{cAMP}/I_{cGMP}	$I_{Ca/CaM}/I$
CNGA1	0.025 ± 0.003 (5)	ND
CNGA1 + CNGB1	0.21 ± 0.02 (12)	0.53 ± 0.004 (4)
CNGA1-eCFP + CNGA1-eYFP	0.050 ± 0.01(4)	0.97 ± 0.05 (3)
CNGA1-eCFP + CNGA1-eYFP + CNGB1	0.14 ± 0.002 (3)	0.53 ± 0.05 (3)
CNGA1 + CNGB1-eCFP + CNGB1-eYFP	0.19 ± 0.06 (3)	0.56 ± 0.01 (3)
CNGA1 + eCFP-CNGB1 + eYFP-CNGB1	0.20 ± 0.06 (4)	0.49 ± 0.02 (3)
CNGA1-eCFP + eYFP-CNGB1	0.29 ± 0.07 (4)	0.56 ± 0.07 (3)
Native rod CNG channel	0.2–0.4[a]	0.5[b]

Ratio of the current activated by saturating cAMP to the current activated by saturating cGMP (I_{cAMP}/I_{cGMP}), and the current activated by subsaturating cGMP in the presence of Ca^{2+}/CaM to the current in the absence of Ca^{2+}/CaM ($I_{Ca/CaM}/I$). Currents were measured at +60 mV, and ratios are expressed as mean ± SEM (n).

[a] Picco et al., 1996; Tanaka et al., 1989

[b] Gordon et al., 1995; Rebrik and Korenbrot, 1998

eYFP-CNGB1). The eCFP and eYFP-containing channels exhibited functional behavior indistinguishable from channels without fluorescence proteins attached (see Table 1). They were made with a PCR-based method and confirmed with fluorescence-based sequencing. The cDNAs were subcloned into the pGEMHE vector (a gift from E. Liman) for expression in *Xenopus* oocytes. RNA for oocyte injection was made with the Message Machine kit (Ambion, Austin, TX).

Xenopus oocytes were microinjected with a mixture of CNG channel RNAs and incubated for 5–8 days at 16°C prior to recording. An RNA ratio of 1:4 was used for coexpression of CNGA1 and CNGB1 subunits. This produced a pure population of heteromeric channels (Shammat and Gordon, 1999), which was confirmed with functional measurements (Figure 3, Table 1). An RNA ratio of 2:1 was generally used for coexpression of eCFP and eYFP constructs. The excess eCFP-tagged subunits ensured that each eYFP-tagged subunit was next to an eCFP-tagged subunit and contributed to FRET during energy transfer. Incorporation of each subunit type was confirmed by fluorescence intensity from the fluorescent protein attached to the subunit, as well as by electrophysiological properties (Figure 3, Table 1).

The electrophysiological recordings from the oocytes were done as previously described (Trudeau and Zagotta, 2002a). Macroscopic ionic currents were recorded in the inside-out configuration of the patch-clamp technique using an Axopatch 200A patch-clamp amplifier (Axon Instruments, Foster City, CA) and digitized with an ITC-16 computer interface (Instrutech, Great Neck, NY). Currents were recorded with consecutive 300 ms voltage steps to −60 mV and +60 mV in the presence of the indicated solution, and the leak current in the absence of cyclic nucleotide was subtracted. Data were acquired and analyzed with PULSE software (HEKA) with additional analysis using IGOR software (Wavemetrics, Lake Oswego, OR) running on a Pentium PC. Internal (bath) solutions were applied with an RSC-100 solution changer (Molecular Kinetics, Pullman, WA) and contained 130 mM NaCl, 3 mM HEPES, 0.2 mM EDTA (pH 7.2). Cyclic nucleotides (cAMP and cGMP) were added to the internal solution at the concentration given in the text. The external (pipette) solution was identical to the internal solution but contained 500 μM niflumic acid to inhibit endogenous chloride channels. For internal solutions with Ca^{2+} or Ca^{2+}/CaM, EDTA was replaced with 0.2 mM nitriloacetic acid and $CaCl_2$ was added to give a free Ca^{2+} concentration of 1 μM (Trudeau and Zagotta, 2002b). Calmodulin (Calbiochem) was added at a concentration of 250 nM. All chemicals were from Sigma, unless noted.

Fluorescence signals were collected from the animal pole of oocytes under a confocal microscope (Leica), using laser excitation at 458 nm and 488 nm and an emission window of 5 nm. Background contamination was quantified from the blank area and subtracted when constructing spectra. The spectra closely matched the published spectra for these mutant GFP variants (Heim and Tsien, 1996), suggesting that the fluorescent proteins retained their fluorescence properties as fusion proteins with CNG channels. Under the same condition, uninjected oocytes or oocytes expressing CNG channels without fluorescent tags yielded very low endogenous fluorescence with different spectral properties (see Figure 3). Furthermore, oocytes injected with eCFP and eYFP fused to two noninteracting membrane proteins, a CNG channel subunit and the cannabinoid receptor CB1, respectively, showed no FRET signal (data not shown). A narrow range of PMT gain was used to ensure linearity, which was checked by calculating FRET efficiency in a wavelength range covering both strong and weak eYFP emission (see Figures 1D and 1E).

Quantification of FRET efficiency between eCFP and eYFP is complicated by the fact that, in general, emission at the acceptor wavelength contains three components: eYFP emission due to FRET, eYFP emission due to direct excitation at 458 nm, and eCFP emission. We chose a spectra approach to remove contaminations due to donor emission and direct excitation of the acceptor (see Figures 1B and 1C). This method also eliminated errors arising from variation in the quantum yield of the acceptor or in the concentration of total fluorescence molecules (Clegg, 1992; Selvin, 1995). An eCFP spectrum collected from eCFP-containing channels (CNGA1-eCFP) was recorded and used to subtract the component of eCFP emission from spectra taken from eCFP/eYFP samples with 458 nm excitation. This yielded a subtracted eYFP emission spectrum, F_{458}, that had two components: one due to direct excitation, F_{458}^{direct}, and one due to FRET, F_{458}^{FRET}. F_{458} was normalized by the eYFP emission with 488 nm excitation, F_{488}. The resulted ratio, termed RatioA, can be expressed as

$$RatioA = \frac{F_{458}}{F_{488}} = \frac{F_{458}^{direct}}{F_{488}} + \frac{F_{458}^{FRET}}{F_{488}}$$

The direct excitation component, F_{458}^{direct}/F_{488}, termed $RatioA_0$, was experimentally determined with eYFP-containing channels (CNGA1-eYFP). The difference between RatioA and $RatioA_0$ is directly proportional to FRET efficiency.

Acknowledgments

We are grateful to Heidi Utsugi, Kevin Black, Gay Sheridan, and Shellee Cunnington for technical assistance, to Paulette Brunner of the Keck Imaging Center for help with confocal microscopy, and to members of the Zagotta lab for insightful discussions. This work was supported by the Howard Hughes Medical Institute and a grant from the National Eye Institute (EY10329) to W.N.Z.

Received: November 3, 2002
Revised: November 13, 2002
Published online: November 20, 2002

References

Bauer, P.J. (1996). Cyclic GMP-gated channels of bovine rod photoreceptors: affinity, density and stoichiometry of Ca(2+)-calmodulin binding sites. J. Physiol. *494*, 675–685.

Bonigk, W., Bradley, J., Muller, F., Sesti, F., Boekhoff, I., Ronnett,

G.V., Kaupp, U.B., and Frings, S. (1999). The native rat olfactory cyclic nucleotide-gated channel is composed of three distinct subunits. J. Neurosci. *19*, 5332–5347.

Bradley, J., Li, J., Davidson, N., Lester, H.A., and Zinn, K. (1994). Heteromeric olfactory cyclic nucleotide-gated channels: a subunit that confers increased sensitivity to cAMP. Proc. Natl. Acad. Sci. USA *91*, 8890–8894.

Bradley, J., Zhang, Y., Bakin, R., Lester, H.A., Ronnett, G.V., and Zinn, K. (1997). Functional expression of the heteromeric "olfactory" cyclic nucleotide-gated channel in the hippocampus: a potential effector of synaptic plasticity in brain neurons. J. Neurosci. *17*, 1993–2005.

Bradley, J., Reuter, D., and Frings, S. (2001). Facilitation of calmodulin-mediated odor adaptation by cAMP-gated channel subunits. Science *294*, 2176–2178.

Chen, T.Y., Peng, Y.W., Dhallan, R.S., Ahamed, B., Reed, R.R., and Yau, K.W. (1993). A new subunit of the cyclic nucleotide-gated cation channel in retinal rods. Nature *362*, 764–767.

Chen, T.Y., Illing, M., Molday, L.L., Hsu, Y.T., Yau, K.W., and Molday, R.S. (1994). Subunit 2 (or beta) of retinal rod cGMP-gated cation channel is a component of the 240-kDa channel-associated protein and mediates Ca(2+)-calmodulin modulation. Proc. Natl. Acad. Sci. USA *91*, 11757–11761.

Clegg, R.M. (1992). Fluorescence resonance energy transfer and nucleic acids. Methods Enzymol. *211*, 353–388.

Doyle, D.A., Morais Cabral, J., Pfuetzner, R.A., Kuo, A., Gulbis, J.M., Cohen, S.L., Chait, B.T., and MacKinnon, R. (1998). The structure of the potassium channel: molecular basis of K+ conduction and selectivity. Science *280*, 69–77.

Gordon, S.E., Downing-Park, J., and Zimmerman, A.L. (1995). Modulation of the cGMP-gated ion channel in frog rods by calmodulin and an endogenous inhibitory factor. J. Physiol. *486*, 533–546.

He, Y., Ruiz, M., and Karpen, J.W. (2000). Constraining the subunit order of rod cyclic nucleotide-gated channels reveals a diagonal arrangement of like subunits. Proc. Natl. Acad. Sci. USA *97*, 895–900.

Heim, R., and Tsien, R.Y. (1996). Engineering green fluorescent protein for improved brightness, longer wavelengths and fluorescence resonance energy transfer. Curr. Biol. *6*, 178–182.

Hsu, Y.T., and Molday, R.S. (1993). Modulation of the cGMP-gated channel of rod photoreceptor cells by calmodulin. Nature *361*, 76–79.

Hsu, Y.T., and Molday, R.S. (1994). Interaction of calmodulin with the cyclic GMP-gated channel of rod photoreceptor cells. Modulation of activity, affinity purification, and localization. J. Biol. Chem. *269*, 29765–29770.

Kaupp, U.B., Niidome, T., Tanabe, T., Terada, S., Bonigk, W., Stuhmer, W., Cook, N.J., Kangawa, K., Matsuo, H., Hirose, T., et al. (1989). Primary structure and functional expression from complementary DNA of the rod photoreceptor cyclic GMP-gated channel. Nature *342*, 762–766.

Korschen, H.G., Illing, M., Seifert, R., Sesti, F., Williams, A., Gotzes, S., Colville, C., Muller, F., Dose, A., Godde, M., et al. (1995). A 240 kDa protein represents the complete beta subunit of the cyclic nucleotide-gated channel from rod photoreceptor. Neuron *15*, 627–636.

Liman, E.R., and Buck, L.B. (1994). A second subunit of the olfactory cyclic nucleotide-gated channel confers high sensitivity to cAMP. Neuron *13*, 611–621.

Liu, D.T., Tibbs, G.R., Paoletti, P., and Siegelbaum, S.A. (1998). Constraining ligand-binding site stoichiometry suggests that a cyclic nucleotide-gated channel is composed of two functional dimers. Neuron *21*, 235–248.

Miyawaki, A., Llopis, J., Heim, R., McCaffery, J.M., Adams, J.A., Ikura, M., and Tsien, R.Y. (1997). Fluorescent indicators for Ca^{2+} based on green fluorescent proteins and calmodulin. Nature *388*, 882–887.

Munger, S.D., Lane, A.P., Zhong, H., Leinders-Zufall, T., Yau, K.W., Zufall, F., and Reed, R.R. (2001). Central role of the CNGA4 channel subunit in Ca^{2+}-calmodulin-dependent odor adaptation. Science *294*, 2172–2175.

Patterson, G.H., Piston, D.W., and Barisas, B.G. (2000). Forster distances between green fluorescent protein pairs. Anal. Biochem. *284*, 438–440.

Picco, C., Sanfilippo, C., Gavazzo, P., and Menini, A. (1996). Modulation by internal protons of native cyclic nucleotide-gated channels from retinal rods. J. Gen. Physiol. *108*, 265–276.

Rebrik, T.I., and Korenbrot, J.I. (1998). In intact cone photoreceptors, a Ca^{2+}-dependent, diffusible factor modulates the cGMP-gated ion channels differently than in rods. J. Gen. Physiol. *112*, 537–548.

Sautter, A., Zong, X., Hofmann, F., and Biel, M. (1998). An isoform of the rod photoreceptor cyclic nucleotide-gated channel beta subunit expressed in olfactory neurons. Proc. Natl. Acad. Sci. USA *95*, 4696–4701.

Selvin, P.R. (1995). Fluorescence resonance energy transfer. In Methods in Enzymology, R. Wu, ed. (San Diego, CA: Academic Press, Inc.), pp. 300–334.

Shammat, I.M., and Gordon, S.E. (1999). Stoichiometry and arrangement of subunits in rod cyclic nucleotide-gated channels. Neuron *23*, 809–819.

Tanaka, J.C., Eccleston, J.F., and Furman, R.E. (1989). Photoreceptor channel activation by nucleotide derivatives. Biochemistry *28*, 2776–2784.

Trudeau, M.C., and Zagotta, W.N. (2002a). An intersubunit interaction regulates trafficking of rod cyclic nucleotide-gated channels and is disrupted in an inherited form of blindness. Neuron *34*, 197–207.

Trudeau, M.C., and Zagotta, W.N. (2002b). Mechanism of calcium/calmodulin inhibition of rod cyclic nucleotide-gated channels. Proc. Natl. Acad. Sci. USA *99*, 8424–8429.

Yau, K.W., and Baylor, D.A. (1989). Cyclic GMP-activated conductance of retinal photoreceptor cells. Annu. Rev. Neurosci. *12*, 289–327.

Zagotta, W.N., and Siegelbaum, S.A. (1996). Structure and function of cyclic nucleotide-gated channels. Annu. Rev. Neurosci. *19*, 235–263.